Floquet-Bloch Oscillations and Intraband Zener Tunneling in an Oblique Spacetime Crystal

Qiang Gao and Qian Niu
Department of Physics, The University of Texas at Austin, Austin, Texas 78712, USA

(Received 20 December 2020; accepted 21 June 2021; published 14 July 2021)

We study an oblique spacetime crystal realized by a monoatomic crystal in which a sound wave propagates, and analyze its quasienergy band structure starting from a tight-binding Bloch band for the static crystal. We investigate Floquet-Bloch oscillations under an external field, which show different characteristics for different band topologies. We also discover intraband Zener tunneling beyond the adiabatic limit, which effectively converts between different band topologies. Our results indicate the possibility of energy conversion between the sound wave and a dc electric field.

DOI: 10.1103/PhysRevLett.127.036401

Introduction.—Periodically driven quantum systems have a long history of study in physics, and have emerged in recent years as a new playground for novel topological properties [1–3] and quantum materials engineering [4]. There are also discussions on the tantalizing possibility of the spontaneous formation of time crystals [5–8] and spacetime crystals [9], adding new excitements to this field. However, there is still much to be explored, and there are challenges in understanding the electronic dynamics in such systems [10,11].

According to a recently reported symmetry classification [12], spacetime crystals fall into rectangular and oblique categories, depending on whether the system has separate translational symmetries in space and time. Here, we present an example for the latter, a monoatomic crystal in which a single mode of sound wave propagates. One can still make a Floquet-Bloch analysis, but quasienergies and momenta are now defined modulo an oblique Brillouin zone, and the usual concepts of Bloch oscillations and Zener tunneling for Bloch bands can be essentially modified. We find Floquet-Bloch oscillations unraveling unusual types of band topologies. We then discuss intraband Zener tunneling, which cannot occur for a rectangular spacetime crystal, and the adiabatic conditions for the validation of realizing one particular band topology. Our results indicate a novel mechanism for a quantum acousto-electric generator that converts energy between the sound wave and a dc electric field.

Floquet-Bloch analysis for an oblique spacetime crystal.—The oblique spacetime crystal considered here is a monoatomic crystal with sound waves propagating through it:

$$H(\boldsymbol{x},t)=\frac{-\hbar^2}{2M}\nabla_x^2+\sum_{\boldsymbol{R}}V(\boldsymbol{x}-\tilde{\boldsymbol{R}}), \tag{1}$$

with the atomic position being time-dependent $\tilde{\boldsymbol{R}}=\boldsymbol{R}-\boldsymbol{A}\cos(\boldsymbol{\kappa}\cdot\boldsymbol{R}-\Omega t)$. Here, the $(\boldsymbol{\kappa},\Omega)$ is the momentum and frequency of that sound wave, $|\boldsymbol{A}|$ is the oscillation amplitude, and $\boldsymbol{R}=n_1\boldsymbol{a}_1+n_2\boldsymbol{a}_2+n_3\boldsymbol{a}_3$ labels the lattice sites. This Hamiltonian has the following translational symmetries: $H(\boldsymbol{x},t+2\pi/\Omega)=H(\boldsymbol{x},t)=H(\boldsymbol{x}+\boldsymbol{R},t+\boldsymbol{\kappa}\cdot\boldsymbol{R}/\Omega)$, which defines an oblique spacetime lattice with nonorthogonal lattice vectors: $[\boldsymbol{0},(2\pi/\Omega)]$ and $[\boldsymbol{R},(\boldsymbol{\kappa}\cdot\boldsymbol{R}/\Omega)]$. Those vectors determine the reciprocal lattice structure to be also oblique, characterized by vectors: $(\boldsymbol{\kappa},\Omega)$ and $(\boldsymbol{G},0)$, where $\boldsymbol{G}$ is the reciprocal lattice vector of the corresponding static crystal [13]. (When the sound wave vector $\boldsymbol{\kappa}$ is rationally related to $\boldsymbol{G}$, one may adopt a superlattice point of view with a folded Brillouin zone, so that the system may be taken as a rectangular spacetime superlattice, but there will be seemingly "mysterious" band crossings due to the band folding).

The Floquet-Bloch band theory of the oblique spacetime crystal goes quite parallel to that for a rectangular spacetime crystal [14]. The eigenstates that respect periodicities of the Hamiltonian satisfy the time-dependent Schrödinger equation:

$$H(\boldsymbol{x},t)|\Psi(\boldsymbol{x},t)\rangle=i\hbar\partial_t|\Psi(\boldsymbol{x},t)\rangle. \tag{2}$$

We consider that $|\boldsymbol{A}|\ll$ lattice constants and the effect of lattice vibration to leading orders in the amplitude $\boldsymbol{A}$: $H(\boldsymbol{x},t)=H_0(\boldsymbol{x})+\boldsymbol{A}\cdot\boldsymbol{H}_1(\boldsymbol{x},t)+\cdots$, where H_0 is the Hamiltonian of the corresponding static crystal. To simplify matters, we assume that the electrons are all in the lowest Bloch band of the static crystal, which is well separated from all other bands energetically so that mixing with them can be ignored when the lattice vibration is turned on.

Under these conditions, lattice vibrations can still mix a Bloch state $\{|\psi_{\boldsymbol{k}}(\boldsymbol{x})\rangle\}$ of energy $\omega_g(\boldsymbol{k})$ in the lowest band with its phononic "sidebands," which differ with each other

by an integer multiple of the phonon energy and momentum $(\Omega, \boldsymbol{\kappa})$. In other words, we can choose the basis states to be the phonon replica of a Bloch state:

$$\{|\Phi_{n,\boldsymbol{k}}(\boldsymbol{x},t)\rangle \equiv e^{-in\Omega t}|\psi_{\boldsymbol{k}+n\boldsymbol{\kappa}}(\boldsymbol{x})\rangle\}, \tag{3}$$

where n is the replica index. This basis can be made orthonormal under a new inner product defined as

$$\langle\langle\phi(\boldsymbol{x},t)|\psi(\boldsymbol{x},t)\rangle\rangle \equiv \frac{1}{T}\int_0^T dt \int d\boldsymbol{x}\phi^*(\boldsymbol{x},t)\psi(\boldsymbol{x},t), \tag{4}$$

where $T = 2\pi/\Omega$ is the Floquet time period.

Having the phonon replica basis, we can then expand the eigenstate in Eq. (2) as

$$|\Phi_{\omega,\boldsymbol{k}}(\boldsymbol{x},t)\rangle = \sum_n e^{-i\omega t} f_{\boldsymbol{k}}^n |\Phi_{n,\boldsymbol{k}}(\boldsymbol{x},t)\rangle, \tag{5}$$

where $(\omega, \boldsymbol{k})$ are the quasienergy and quasimomentum, respectively. Since those two quantities are conserved modulo a Brillouin zone due to the periodicity in the reciprocal space, we can use them as characterizations for the eigenstates. Utilizing the orthonormal conditions of the basis functions, we then find that the coefficients $f_{\boldsymbol{k}}^n$ satisfy the following matrix eigenvalue equation: $\sum_n \mathcal{H}_{m,n}(\boldsymbol{k}) f_{\boldsymbol{k}}^n = \hbar\omega f_{\boldsymbol{k}}^m$ where the elements of the Kernel matrix $\mathcal{H}(\boldsymbol{k})$ are given by

$$\mathcal{H}_{m,n} \equiv \langle\langle\Phi_{m,\boldsymbol{k}}(\boldsymbol{x},t)|H(\boldsymbol{x},t)|\Phi_{n,\boldsymbol{k}}(\boldsymbol{x},t)\rangle\rangle - \hbar n\Omega\delta_{mn}. \tag{6}$$

In the static limit of $\boldsymbol{A} = \boldsymbol{0}$, the matrix $\mathcal{H}$ is diagonal with eigenvalues $\omega_n(\boldsymbol{k}) = \omega_g(\boldsymbol{k} + n\boldsymbol{\kappa}) - n\Omega$, meaning that the quasienergy bands are just the original Bloch band $\omega_g(\boldsymbol{k})$ shifted by the reciprocal lattice vector $(\boldsymbol{\kappa}, \Omega)$. When lattice vibration is turned on, off-diagonal elements of the Hamiltonian will appear, which can open gaps at places where the Bloch band crosses with its phonon replicas. From the calculation, we also find a general relation between different quasienergy bands:

$$\omega_{n+m}(\boldsymbol{k}) = \omega_m(\boldsymbol{k} + n\boldsymbol{\kappa}) - n\Omega, \tag{7}$$

which reflects the periodicity in the reciprocal space.

These general features of the Floquet-Bloch band structure are illustrated in Fig. 1 for the case of a $(1+1)$ D oblique crystal. The dashed curves are the unperturbed bands with no oscillation, and we can see they are nothing but replicas of the original cosine-shape Bloch band. The solid curves are the band dispersion under time-dependent perturbation. The red shaded area stands for the Brillouin zone of the oblique spacetime crystal characterized by two reciprocal lattice vectors: $(G = 2\pi/a, 0)$ and (κ, Ω). Without loss of physics, we take the region containing the $(n = 0)$ band $\omega_0(k)$ as our first Brillouin zone and all others as replicas.

Floquet-Bloch oscillations and band topology.—Very interesting phenomena such as Bloch oscillations and Zener tunneling can occur for Bloch bands in the presence of an external electric field E, and it is natural to ask what can happen to the quasienergy bands in a spacetime crystal. If we represent the field by a vector potential and treat its time dependence adiabatically, i.e., as very slow compared to all other timescales in the problem, we can still use the quasienergy states as solutions provided that the quasimomentum is replaced as $k \to k - eEt/\hbar$. Then by using the perturbation method, we can find an expression for the group velocity $\dot{x}$. Together with the time-dependent quasimomentum, the electronic motion in a quasienergy band can be summarized as

$$\dot{k} = -\frac{eE}{\hbar}, \qquad \dot{x} = \frac{\partial\omega_n(k)}{\partial k}, \tag{8}$$

which leads to a similar motion as Bloch oscillations that we call Floquet-Bloch oscillations in the present context [20]. Indeed, for the band structure in Fig. 1, the quasienergy is periodic in momentum, $\omega_n(k + 2\pi/a) = \omega_n(k)$, which implies, according to the equations of motion, that the velocity of electrons is also periodic in time with period $(\hbar/eE)G$ [21]. Similar discussion in the time-driven system can be found in Ref. [22].

However, in the oblique spacetime crystal, quasienergy bands can also, in principle, exhibit nontrivial periodicity like $\omega_n(k + \kappa) = \omega_n(k) + \Omega$ or even more exotically $\omega_n(k + 2\pi/a \pm \kappa) = \omega_n(k) \pm \Omega$, which will lead to new oscillation periods of $(\hbar/eE)\kappa$ and $(\hbar/eE)(G \pm \kappa)$, respectively. Those unique behaviors suggest different unusual band topologies [23].

To appreciate the possibilities of different topologies, we project the Brillouin zone onto a torus by shearing it into a rectangle and wrapping around to join the opposite edges. A quasienergy dispersion is then characterized by a pair of winding numbers N_ω and N_k around the two topologically distinct directions represented by the reciprocal lattice vectors $\tilde{\boldsymbol{\omega}} = (\kappa, \Omega)$ and $\boldsymbol{k} = (G, 0)$. One can identify that

$$N_\omega = \frac{i}{2\pi}\int_{BZ} \mathrm{Tr}(U_\omega^\dagger dU_\omega) = \frac{T}{2\pi}\int_{BZ} dk\frac{\partial\omega(k)}{\partial k} \tag{9}$$

is the winding number for the Floquet operator $U_\omega = e^{-i\omega(k)T}$ [24]. Similarly, one can think of N_k as the winding number for the evolution operator along the other spacetime periodic direction $[a, (\kappa a/\Omega)]$:

$$N_k = \frac{-i}{2\pi}\int_{BZ} \mathrm{Tr}(U_k^\dagger dU_k) = \int_{BZ}\left[\frac{a}{2\pi}dk - \frac{T}{2\pi}\kappa a d\omega\right], \tag{10}$$

with $U_k \equiv e^{i[ka-\omega(\kappa a/\Omega)]}$ and an extra "-" for convention. The examples are illustrated in Fig. 2, with $N_\omega = 0, N_k = 1$ for panel (a), $N_\omega = 1, N_k = 0$ in panel (b), and $N_\omega = -1,$

$N_k = 1$ in panel (c), corresponding to the Floquet-Bloch oscillations with periods $\propto N_k G + N_\omega \kappa$.

Although we do not yet find the possibilities illustrated in panels (b) and (c) within the model studied in this work, we discover a system called oscillating Dirac comb that can possess a gapless band structure for a specific oscillation amplitude (with more details given in the Supplemental Material [16]), as shown schematically in panel (d). We have intentionally plotted the band in red and blue corresponding to the topologies in panels (b) and (c), respectively. Taking the band structure as two different topologies requires that the electron cannot be in a superposition of the two segments plotted in blue and red and must remain consistently on one of them when passing through the crossing point.

However, an exact gap closing in the oscillating Dirac comb requires a fine-tuning of parameters [16], which is not robust under any other perturbations and thus unrealistic in real experiments. So, we have to allow such a system to have a tiny gap. In the next section, we will see how the joint topology shown in panel (d) is possible even with a tiny gap opened at the crossing point by discussing the intraband Zener tunneling and the adiabatic conditions.

Intraband Zener tunneling and adiabatic condition.—Zener tunneling refers to the breakdown of adiabaticity when the rate of parameter change cannot be regarded as small compared to the gap between the energy levels, and there is also an analog of the phenomenon between quasienergy levels in Floquet systems [26–28]. In crystals under an electric field, the crystal momentum becomes a time-dependent parameter, and interband Zener tunneling has been well studied. Here, due to the fact that in oblique spacetime crystals, the gaps can be opened between a quasienergy band and its periodic replicas (as shown in Fig. 1), we can actually anticipate an intraband Zener tunneling happening through such gaps.

The analysis of the intraband Zener tunneling is quite similar to that of normal Zener tunneling between different Bloch bands. The key idea is that we consider tunneling between two eigenstates $|\psi_1(k)\rangle$ and $|\psi_2(k)\rangle$:

$$|\psi_1(k)\rangle = \sum_n f_k^n |\Phi_{n,k}(x,t)\rangle,$$
$$|\psi_2(k)\rangle = \sum_n f_{k-\kappa}^n |\Phi_{n-1,k}(x,t)\rangle, \tag{11}$$

sitting on two adjacent bands (replicas) labeled by 1 and 2, which have quasienergies $\epsilon_1 = \omega(k)$ and $\epsilon_2 = \omega(k-\kappa)+\Omega$, respectively, with a direct gap Δ_0. One can check that $|\psi_1(k)\rangle$ and $|\psi_2(k)\rangle$ are orthonormal ($\langle\langle\psi_i(k)|\psi_j(k)\rangle\rangle = \delta_{ij}$). The reason why such tunneling is indeed an intraband process is that $|\psi_2(k)\rangle$ is equivalent to $|\psi_1(k-\kappa)\rangle$ since they differ by a reciprocal lattice vector. The transition between $|\psi_1(k)\rangle$ and $|\psi_1(k-\kappa)\rangle$ then involves a shift in momentum, which is associated with absorption or emission of a quantum of sound mode (Ω, κ).

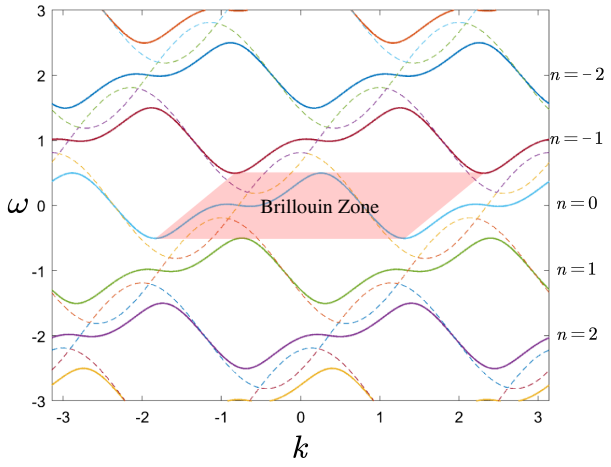

FIG. 1. Floquet-Bloch band structure for the $(1+1)D$ oblique spacetime crystal modeled by Eq. (6), originating from the lowest Bloch band (dashed curves repeated over the Brillouin zone) of the unperturbed system. The quasienergy dispersion (solid curves) is calculated when a single mode of the sound wave is turned on to a finite amplitude [15]. The labels on the right vertical axis are the indices of the replicas of the same single band as defined within the Brillouin zone.

To make the tunneling happen, we apply an electric field E, so that, from the equations of motion in Eq. (8), electrons will move adiabatically along the k axis. The real wave function can be approximated as a linear combination of two eigenstates: $|\Phi(t)\rangle = C_1(t)|\psi_1[k(t)]\rangle + C_2(t)|\psi_2[k(t)]\rangle$. In the context of oblique spacetime crystals, such expansion is valid under a vertical (or irrational) basis representation [16].

Now, plugging the wave function $|\Phi(t)\rangle$ into the time-dependent Schrödinger equation, we obtain the following differential equation regarding $C_{1,2}$:

$$i\hbar\frac{\partial}{\partial t}\begin{bmatrix}C_1\\C_2\end{bmatrix} - eE\begin{bmatrix}\mathcal{A}_{11} & \mathcal{A}_{12}\\ \mathcal{A}_{21} & \mathcal{A}_{22}\end{bmatrix}\begin{bmatrix}C_1\\C_2\end{bmatrix} = \begin{bmatrix}\epsilon_1 & 0\\ 0 & \epsilon_2\end{bmatrix}\begin{bmatrix}C_1\\C_2\end{bmatrix}, \tag{12}$$

where $\mathcal{A}_{mn} \equiv \langle\langle\psi_m[k(t)]|(i\partial_k + x)|\psi_n[k(t)]\rangle\rangle$ is the multiband Floquet-type Berry connection. This result has the same form as in Bloch crystals but with modified Berry connections. For spacetime crystal, $\mathcal{A}_{mn}$ generically has two contributions:

$$\mathcal{A}_{mn} = i\sum_l (f_n)^* \partial_k f_m + \sum_l (f_n)^* f_m \mathcal{A}_{k+lk}, \tag{13}$$

where $f_1 \to f_k^l$ and $f_2 \to f_{k-\kappa}^{l+1}$. The first term is the Floquet contribution, while the second term is the modified Bloch contribution with $\mathcal{A}_{k+lk}$ being the usual Berry connection. For the Floquet-Bloch system generated by a single Bloch band well separated from all other bands, this Bloch contribution is numerically small and negligible. Then $\mathcal{A}_{mn}(k)$ has only the Floquet contribution that comes

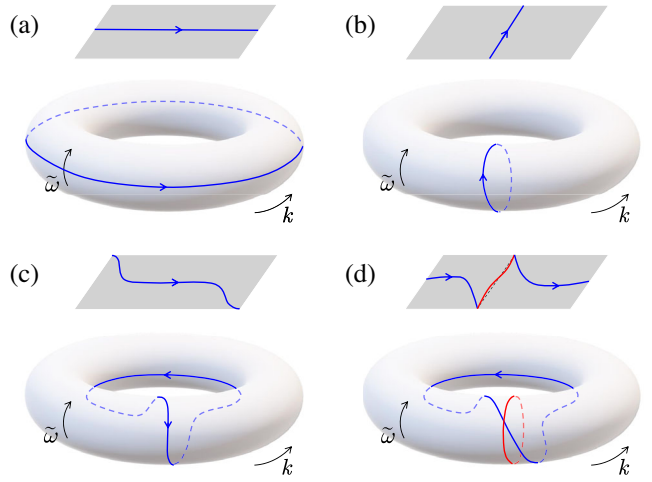

FIG. 2. The topology of band dispersions (blue curves) as seen in the Brillouin zone and on the torus after shearing it and wrapping around along the reciprocal lattice vectors: $\tilde{\boldsymbol{\omega}} = (\kappa, \Omega)$ and $\boldsymbol{k} = (G, 0)$. (a) Corresponds to the class shown in Fig. 1. (b) Is a class that has yet to be seen and is only possible in oblique spacetime crystals [25]. (c) Corresponds to typical edge states of topological Floquet insulator in a higher dimension [3]. (d) Shows to a unique gapless band structure that combines the topologies in both (b),(c).

solely from the time variations, which allows us to consider only the kernel $\mathcal{H}(k)$ in Eq. (6).

We again use the oscillating Dirac comb but now with a small gap as an example to show some numerical results. Figure 3(a) shows the band structure of such a system, which resembles a so-called Landau-Zener grid [22,29]. We then numerically solve Eq. (12) near the gap at point B in Fig. 3(a), with the electron initially sitting on band ϵ_1 ($C_1 = 1$, $C_2 = 0$). The squared moduli $|C_1|^2$ and $|C_2|^2$ as functions of k under different external field strengths are plotted in Fig. 3(b) using dashed and solid curves, respectively. We can see that when $|eE| = 10^{-3}$ eV/Å (blue curves), the evolutions of $|C_{1,2}|^2$ are close to step functions indicating total tunneling through the gap, while for larger $|eE|$, the electron is in a superposition of two bands, violating the adiabaticity. Such violation comes from a larger direct gap near the gap at point B, which mixes two bands too early. This tells us that when $|eE|$ is small enough, we can just ignore the influences of that larger gap and only consider the behavior of electron at the vicinity of point B, allowing us to have an analytic discussion.

The system near the point B can be asymptotically approximated by a two-level system as

$$h(k) = \begin{bmatrix} \mathcal{E}_2(k) & \Delta_0/2 \\ \Delta_0/2 & \mathcal{E}_1(k) \end{bmatrix}, \tag{14}$$

where Δ_0 is the gap at $k = k_B$, and $\mathcal{E}_{1,2}(k) = \mu_{1,2}(k - k_B)$ are the asymptotes of bands ϵ_1 and ϵ_2 near the gap. Thus, we end up with Zener's original tunneling model with a transition rate [30]:

$$\Gamma = \exp\left(-\frac{\pi\Delta_0^2}{2eE|\mu_1 - \mu_2|}\right). \tag{15}$$

In Fig. 3(c), we compare the numerical results with Eq. (15), which are in good agreement with each other when $|eE| \leq 1.5 \times 10^{-3}$ eV/Å. However, as $|eE|$ is getting bigger, the discrepancies occur due to the nonadiabaticity of the states before reaching the gap at point B.

As discussed in last section, for band structure in Fig. 3(a) [or Fig. 2(d) if $\Delta_0 = 0$] to have separate topologies, we need the adiabatic condition when electrons are away from the gap (or the band crossing point) and total tunneling when passing through the gap (or the

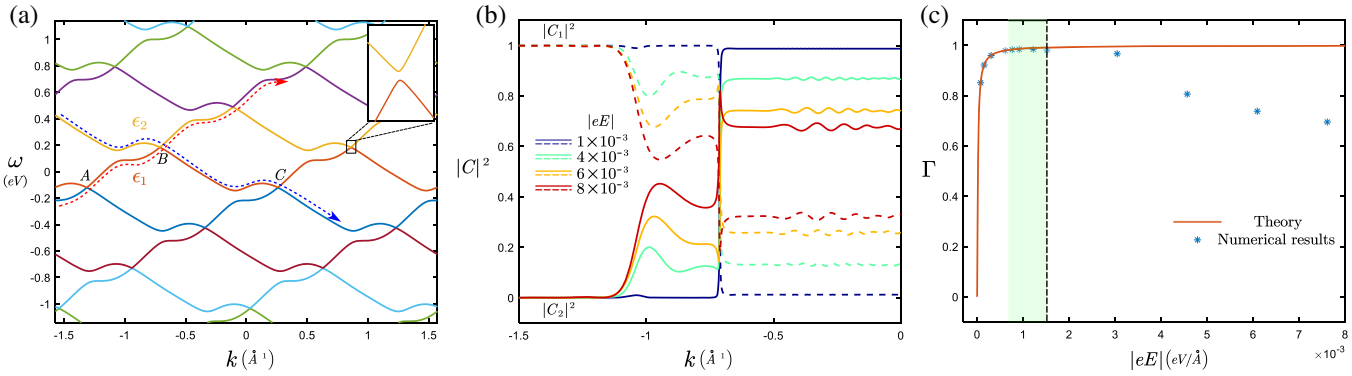

FIG. 3. (a) Floquet-Bloch band structure with a very small gap of avoided crossing, calculated for the example of an oscillating Dirac comb with oscillation amplitude $A = 0.15$ [16], with A, B, and C labeling three typical points. The blue and red dotted curves represent two paths with different topologies also illustrated in Fig. 2(d). (b) The numerical results of the tunneling process between two bands near the point B in panel (a) by solving Eq. (12) with initial conditions $C_1 = 1$ and $C_2 = 0$ under different external field strengths. (c) The numerical results (stars) and the theory from Eq. (15) (curve) of the tunneling rate of the electron from band 1 to 2. The green shade highlights the area where the tunneling rate is approximately one.

crossing point), which requires the tunneling rate to be one at the point B and zero elsewhere. That can be realized when $|eE|$ is in the green shaded area in Fig. 3(c).

Discussion.—Assuming an ideal condition where the tunneling rate is nearly one under a proper electric field E, the electron can then move freely along the red or the blue dotted paths shown in Fig. 3(a), depending on its initial positions, which correspond to the Floquet-Bloch oscillations with periods of $(\hbar/eE)\kappa$ and $(\hbar/eE)(G-\kappa)$, respectively. Such behaviors show a possibility of energy conversion between the sound and an external electric field. The energy involved is actually the energy averaged over one Floquet period T: $\bar{\varepsilon} \equiv \langle\langle H \rangle\rangle$ [16].

To see how the energy is converted, we now restrict our consideration within the Brillouin zone, which is the energy dispersion from point A to B and to C in Fig. 3(a). We must keep in mind that this system only has one band and all others are just replicas. Imaging one electron sitting initially on the segment BC and driven adiabatically from point B to C by $|eE|$. Then at point C, the electron will tunnel through the gap to an adjacent state on the lower band that is equivalent to the state at point B, since they differ by a reciprocal lattice vector. In other words, this is tunneling from point C to point B on a single band associated with absorption of a quantum of sound mode, which is the essence of the intraband Zener tunneling. After a full oscillation period, the electron goes back to its original electronic state (Floquet-Bloch state with the same or equivalent k) but has a net position change:

$$\Delta x|_{k_B}^{k_C} = \int_{t_B}^{t_C} \dot{x} dt = \int_{k_B}^{k_C} \frac{\partial \omega(k)}{\partial k} \frac{dk}{\dot{k}} = -\frac{\hbar(\omega_C - \omega_B)}{eE} \tag{16}$$

indicating a gain in the electric potential energy of the electron. That amount of energy must come from the sound wave since there is no change in the electronic state [16]. When the electron is initially at AB, the process is similar but reversed. We note that a similar process can happen in other Floquet systems [19].

However, in the above analysis, we simplify our considerations by assuming $\Gamma \sim 1$ and excluding other possible scattering channels of the electron. We should anticipate that in a real physical system, the efficiency of the proposed energy conversion could be significantly less than one. In experiments, one can see if the energy conversion is happening by detecting nontrivial Floquet-Bloch oscillation patterns through measuring the ac part of the electric current j induced by the electric field.

The work is supported by NSF (EFMA-1641101) and Welch Foundation (F-1255).

[1] M. C. Rechtsman, J. M. Zeuner, Y. Plotnik, Y. Lumer, D. Podolsky, F. Dreisow, S. Nolte, M. Segev, and A. Szameit, Photonic Floquet topological insulators, Nature (London) **496**, 196 (2013).

[2] N. H. Lindner, G. Refael, and V. Galitski, Floquet topological insulator in semiconductor quantum wells, Nat. Phys. **7**, 490 (2011).

[3] S. Yao, Z. Yan, and Z. Wang, Topological invariants of Floquet systems: General formulation, special properties, and Floquet topological defects, Phys. Rev. B **96**, 195303 (2017).

[4] T. Oka and S. Kitamura, Floquet engineering of quantum materials, Annu. Rev. Condens. Matter Phys. **10**, 387 (2019).

[5] F. Wilczek, Quantum Time Crystals, Phys. Rev. Lett. **109**, 160401 (2012).

[6] D. V. Else, B. Bauer, and C. Nayak, Floquet Time Crystals, Phys. Rev. Lett. **117**, 090402 (2016).

[7] J. Zhang *et al.*, Observation of a discrete time crystal, Nature (London) **543**, 217 (2017).

[8] S. Autti, V. B. Eltsov, and G. E. Volovik, Observation of a Time Quasicrystal and Its Transition to a Superfluid Time Crystal, Phys. Rev. Lett. **120**, 215301 (2018).

[9] T. Li, Z.-X. Gong, Z.-Q. Yin, H. T. Quan, X. Yin, P. Zhang, L.-M. Duan, and X. Zhang, Spacetime Crystals of Trapped Ions, Phys. Rev. Lett. **109**, 163001 (2012).

[10] M. Genske and A. Rosch, Floquet-Boltzmann equation for periodically driven Fermi systems, Phys. Rev. A **92**, 062108 (2015).

[11] M. Messer, K. Sandholzer, F. Görg, J. Minguzzi, R. Desbuquois, and T. Esslinger, Floquet Dynamics in Driven Fermi-Hubbard Systems, Phys. Rev. Lett. **121**, 233603 (2018).

[12] S. Xu and C. Wu, Spacetime Crystal and Spacetime Group, Phys. Rev. Lett. **120**, 096401 (2018).

[13] Because of the convention of quantum mechanics that we always write the propagating phase factor as $e^{i\boldsymbol{k}\cdot\boldsymbol{x}-i\omega t}$, the space and time have naturally different signatures encoded. In this Letter, the signature is set to be $(+,+,+;-)$ where the last entry stands for time. Then we can check that the reciprocal lattice vectors indeed fulfill $-[\boldsymbol{0},(2\pi/\Omega)]\cdot(\boldsymbol{\kappa},\Omega) = [\boldsymbol{R},(\boldsymbol{\kappa}\cdot\boldsymbol{R}/\Omega)]\cdot(\boldsymbol{G},0) = 2\pi$ and $[\boldsymbol{0},(2\pi/\Omega)]\cdot(\boldsymbol{G},0) = [\boldsymbol{R},(\boldsymbol{\kappa}\cdot\boldsymbol{R}/\Omega)]\cdot(\boldsymbol{\kappa},\Omega) = 0$.

[14] A. Gómez-León and G. Platero, Floquet-Bloch Theory and Topology in Periodically Driven Lattices, Phys. Rev. Lett. **110**, 200403 (2013).

[15] The system for obtaining the typical Floquet-Bloch band structure in Fig. 1 is a kernel matrix in Eq. (6) with the diagonal elements being shifted "cos"-shape band dispersion: $\mathcal{H}_{n,n} = 2\beta\cos[(k+n\kappa)a] - n\Omega$, and with the only nonzero off-diagonal terms being $\mathcal{H}_{n,n\pm1} = \delta$. The parameters used are $a = 2$, $\kappa = \Omega = 1$, $\beta = 0.4$, and $\delta = 0.3$.

[16] See Supplemental Material at http://link.aps.org/supplemental/10.1103/PhysRevLett.127.036401 for detailed discussions, which includes Refs. [17–19].

[17] J. von Neumann and E. P. Wigner, Über das Verhalten von Eigenwerten bei adiabatischen Prozessen, Phys. Z. **30**, 467 (1929).

[18] L. D. Landau and E. M. Lifshitz, *Quantum Mechanics: Non-Relativistic Theory* (Elsevier, New York, 2013), Vol. 3.

[19] I. Martin, G. Refael, and B. Halperin, Topological Frequency Conversion in Strongly Driven Quantum Systems, Phys. Rev. X **7**, 041008 (2017).

[20] M. P. Marder, *Condensed Matter Physics* (John Wiley & Sons, New York, 2010).
[21] M. B. Dahan, E. Peik, J. Reichel, Y. Castin, and C. Salomon, Bloch Oscillations of Atoms in an Optical Potential, Phys. Rev. Lett. **76**, 4508 (1996).
[22] A. Gagge and J. Larson, Bloch-like energy oscillations, Phys. Rev. A **98**, 053820 (2018).
[23] This is equivalent to saying that $\omega_n(k) = \omega_n(k+\kappa) - \Omega = \omega_{n+1}(k)$ which means that $\omega_n(k) \equiv \omega_0(k)$ for all n. Later, we will discuss that it requires a very unique band topology depicted in Fig. 2(b).
[24] M. Genske, *Periodically Driven Many-Body Quantum Systems: Quantum Ratchets, Topological States and the Floquet-Boltzmann Equation* (Universität zu Köln, 2017).
[25] Figure 2(b) represents a band topology with $\omega_n(k+\kappa) = \omega_n(k) + \Omega$. If $\kappa = 0$ which corresponds to a rectangular spacetime crystal, then there must be a point on the band such that $\dot{x} = \{[\partial\omega_n(k)]/\partial k\} \to \infty$, which is forbidden by mechanics.
[26] H. P. Breuer and M. Holthaus, Quantum phases and Landau-Zener transitions in oscillating fields, Phys. Lett. **140A**, 507 (1989).
[27] K. Hijii and S. Miyashita, Symmetry for the nonadiabatic transition in Floquet states, Phys. Rev. A **81**, 013403 (2010).
[28] M. Rodriguez-Vega, M. Lentz, and B. Seradjeh, Floquet perturbation theory: Formalism and application to low-frequency limit, New J. Phys. **20**, 093022 (2018).
[29] Yu N. Demkov and V. N. Ostrovsky, Non-adiabatic crossing of energy levels, J. Phys. B **28**, 403 (1995).
[30] C. Zener, Non-adiabatic crossing of energy levels, Proc. R. Soc. A **137**, 696 (1932).